EFFECT OF CONJUGATE HEAT TRANSFER ON THE SIMULATION OF FLOW AT SUPERCRITICAL PRESSURE

Jundi He[1,*], Bing Xu[2], Shuisheng He[1]

[1]Department of Mechanical Engineering, University of Sheffield, United Kingdom, S1 3JD
[2]EDF Energy, Barnett Way, Barnwood, Gloucester, UK, GL4 3RS

ABSTRACT

Direct numerical simulations of upward heated pipe flows of supercritical CO_2 at $Re_0 = 3600$ were carried out to investigate the effect of conjugate heat transfer. Simulation results have good agreement in comparison with those from an earlier experiment [1]. It was found that with the solid pipe wall conduction included in the computational model, enthalpy fluctuations close to the wall is largely dampened and wall heat flux is no longer uniformly distributed. Such changes have a minor effect on flow development and turbulence, but they result in some differences in the heat transfer at the early stage of the flow. The Nusselt number (Nu) has a stronger laminar contribution and a weaker turbulent contribution when the thermal conduction of the solid wall is considered, which results in a larger Nu at an early stage but a lower Nu at a later stage compared with the flow case without a solid wall.

1 INTRODUCTION

A fluid at supercritical pressure does not change phase as temperature increases. However, as the temperature crosses the pseudo-critical value, the fluid changes from liquid-like to gas-like, with significant variations in thermophysical properties. Such special features make supercritical fluid a good working fluid in some industry applications, e.g., the Supercritical-Water-Cooled Reactor—a type of advanced nuclear reactor, supercritical CO_2 power cycles for extracting geothermal energy or the solar energy, carbon capture and storage system and the cooling system of aircraft engines. In a heated flow of supercritical fluid, drastic changes in thermophysical properties can cause abnormal changes in turbulence and heat transfer. Early experiments [2, 3] found that heat transfer deterioration happens in upward flows when heating is moderate, while heat transfer enhancement happens with a stronger heating. Buoyancy is identified as the key reason behind such abnormal phenomena and empirical correlations have been developed to describe the heat transfer of such flows.

Most experiments focus on heat transfer, and only very few studies provided measurements of turbulence or flow features due to technical difficulties. Several recent high-fidelity numerical studies [4, 5] provided another efficient way to look into the physics of such flows. With the help of direct numerical simulations (DNS), the detailed changes in mean flow and turbulent structures can be identified. However, most numerical studies on heated supercritical fluid flows apply a constant wall heat flux at the fluid-wall boundary. In practice, the near-wall fluctuation of enthalpy and thermophysical properties may be dampened due to the solid wall, which is not considered in such numerical studies. Such dampening effect might cause significant changes in near-wall heat transfer and turbulence, which were investigated in two recent numerical studies [6, 7]. Nemati et al. [6] did a comparison between two forced convection flows of supercritical CO_2, with and without enthalpy fluctuations. The impact of thermal boundary condition on turbulence and heat transfer was found to be significant. The comparison between upward heated channel flows with and without the solid wall was carried out by Pucciarelli et al. [7] for the first time, using large eddy simulations (LES). It was found that the fluctuations in near-wall temperature are strongly reduced, and the peak of turbulent kinetic energy is reduced by about half after considering the solid wall. To further understand such effect, DNS of heated pipe flows of supercritical CO_2 are carried out in the present study with and without the solid wall considered. The heat transfer and flow statistics are analysed herein.

*Corresponding author: Jundi He, jundi.he@sheffield.ac.uk

2 METHODOLOGY

Direct numerical simulations (DNS) are carried out in the present study using an in-house code CHAPSim [8, 9]. It is based on the low Mach number approximation and considering the enthalpy dependent variable thermophysical properties. The central difference scheme is used for spatial discretisation of the Navier-Stokes equations, and the third order explicit Runge-Kutta scheme is used for time discretisation. The energy equation for thermal conduction is solved explicitly for the solid domain, and heat flux is coupled at the interface between the solid and fluid domain.

One of the experiments carried out by Luo [1] with strong heating with Re_0=3600 is chosen to be numerically reproduced in the present study. The chosen case is an upward pipe ($D^* = 0.953\ mm$) flow of CO_2 at 7.6 MPa, with an inlet temperature of 295.15 K and a set wall heat flux of 63 kW/m^2. Four DNS cases are carried out as shown in Table 1. Case NoCHT is a base case without the solid wall considered and a constant wall heat flux is applied. While case CHT has a solid wall ($D^*_{inner} = D^*$, $D^*_{outer} = 2.01\ mm$) of stainless steel (Grade 304) [1] with an equivalent heat source applied uniformly in the solid. The solid heatings in case CHT05 and CHT15 start from different locations to model the effect of electrodes in experiments.

Table 1: Case settings

Case	Heating	Re_0	$T_0^*\ (K)$	$D^*_{inner}\ (mm)$	$D^*_{outer}\ (mm)$
NoCHT	Uniform heat flux at the fluid-wall boundary: $q^*_w = 63kW/m^2$	3600	295.15	0.953	None
CHT	Equivalent heat source at the solid pipe: $q^*_v = 204.85kW/m^3$	3600	295.15	0.953	2.01
CHT05	Solid heat source: $q^*_v = 0kW/m^3$ for $z/D < 5$; $q^*_v = 204.85kW/m^3$ for the rest	3600	295.15	0.953	2.01
CHT15	Solid heat source: $q^*_v = 0kW/m^3$ for $z/D < 5$; $q^*_v = 20.485kW/m^3$ for $5 < z/D < 15$; $q^*_v = 204.85kW/m^3$ for the rest	3600	295.15	0.953	2.01

$q^*_v = 204.85kW/m^3$ is equivalent to $q^*_w = 63kW/m^2$

3 RESULT DISCUSSIONS

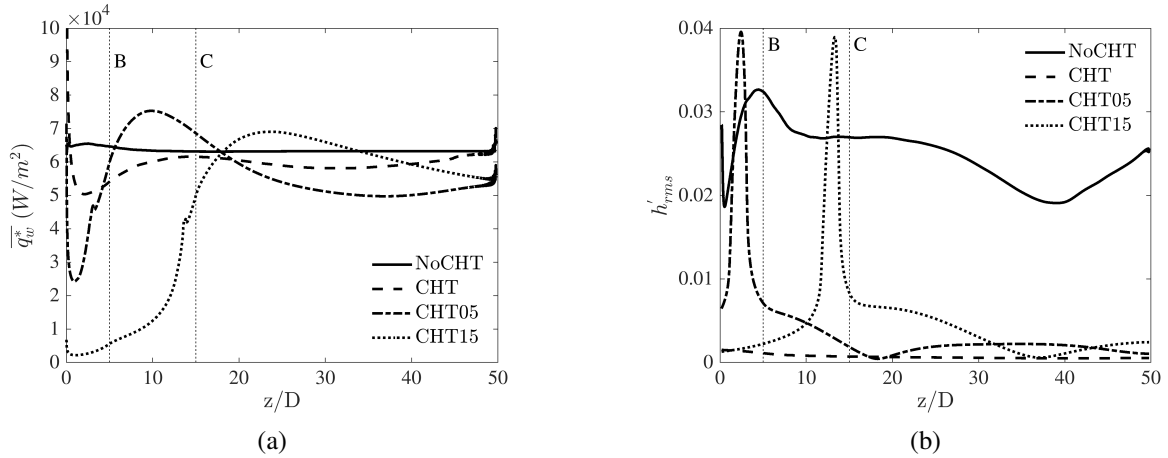

Figure 1: Distributions of wall heat flux (a) and root-mean-square of enthalpy fluctuations close to the wall (y^{+0}=0.043).

Figure 1 shows the wall heat flux and the root-mean-square of enthalpy fluctuation close to the wall in four cases. In comparison with case NoCHT, the wall heat fluxes in the CHT- cases are axially redistributed. In case NoCHT, the level of h'_{rms} is large everywhere along the pipe, whereas h'_{rms} in case CHT05 and CHT15 increases and reduces drastically before the beginning of the solid heating, then they both reduce to a low level. Case CHT has solid heating everywhere and h'_{rms} is low everywhere. h'_{rms} in case NoCHT is about 10 to 20 times of that in case CHT. This may cause changes in heat transfer through the turbulent heat flux and changes in turbulence as the fluctuations in density is dependent on h'_{rms}.

The heat transfer coefficients (HTC) and wall temperatures in the four cases are shown in Figure 2, in comparison with the result from the experiment [1]. It should be noted that the results for cases CHT05 and CHT15 are shifted backward by $5D$ and $15D$, to align the starting locations of heating with other two cases. HTC reduces along the streamwise direction in all cases consistent with the experiment. This is partly due to the thermal boundary development and partly due to the diminished turbulence caused by the combined effect of buoyancy and property variations. HTC of the experiment is between those of case CHT and CHT15 at z/D=10 to 30, but they all agree well after z/D=30. T_w^* increases at streamwise direction in all cases and case CHT has the best agreement with the experiment result.

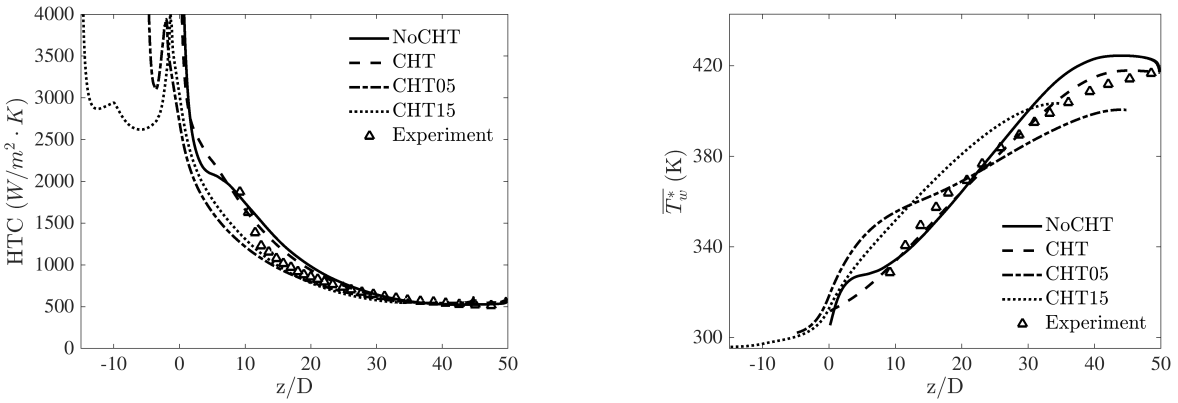

Figure 2: Heat transfer coefficients (a) and wall temperatures (b) of simulations and experiment data.

To study the differences in flow and turbulence, radial profiles of Favre-averaged velocity $\widetilde{u}_z$, turbulent shear stress $\overline{\rho u_z'' u_r''}$ and turbulent kinetic energy $1/2\overline{\rho u_i'' u_i''}$ at several streamwise locations in cases NoCHT and CHT are presented in Figure 3. $\widetilde{u}_z$ and $\overline{\rho u_z'' u_r''}$ in the two cases are nearly the same: The two profiles of $\widetilde{u}_z$ are firstly flattened and become M-shape at later stage, and the two $\overline{\rho u_z'' u_r''}$ profiles reduce quickly and their magnitudes are nearly zero everywhere at $z/D = 35$, where the shear production is minimised. Turbulent kinetic energy in the two cases both reduce quickly and reach the minimum at about $z/D = 25$ and they both start to increase at later stage. This is a typical laminarisation scenario for upward heated flow of supercritical fluid that has been widely studied. The trends are very similar between case NoCHT and CHT except that $\overline{\rho u_z'' u_r''}$ in case CHT has a slightly higher peak at early stage and the peak $1/2\overline{\rho u_i'' u_i''}$ in CHT is slightly higher than that in NoCHT at early stage, but lower after $z/D = 25$. The comparisons suggests that even though h'_{rms} and ρ'_{rms} are significantly different close to the wall in cases NoCHT and CHT, the effect on turbulence during the laminarisation process is rather minor.

Figure 4 shows the radial profiles of enthalpy $\widetilde{h}$, root-mean-square of density fluctuations ρ'_{rms} and radial turbulent heat flux $-\overline{\rho u_r'' h''}$ in the two cases. To present the differences close to the wall, h and

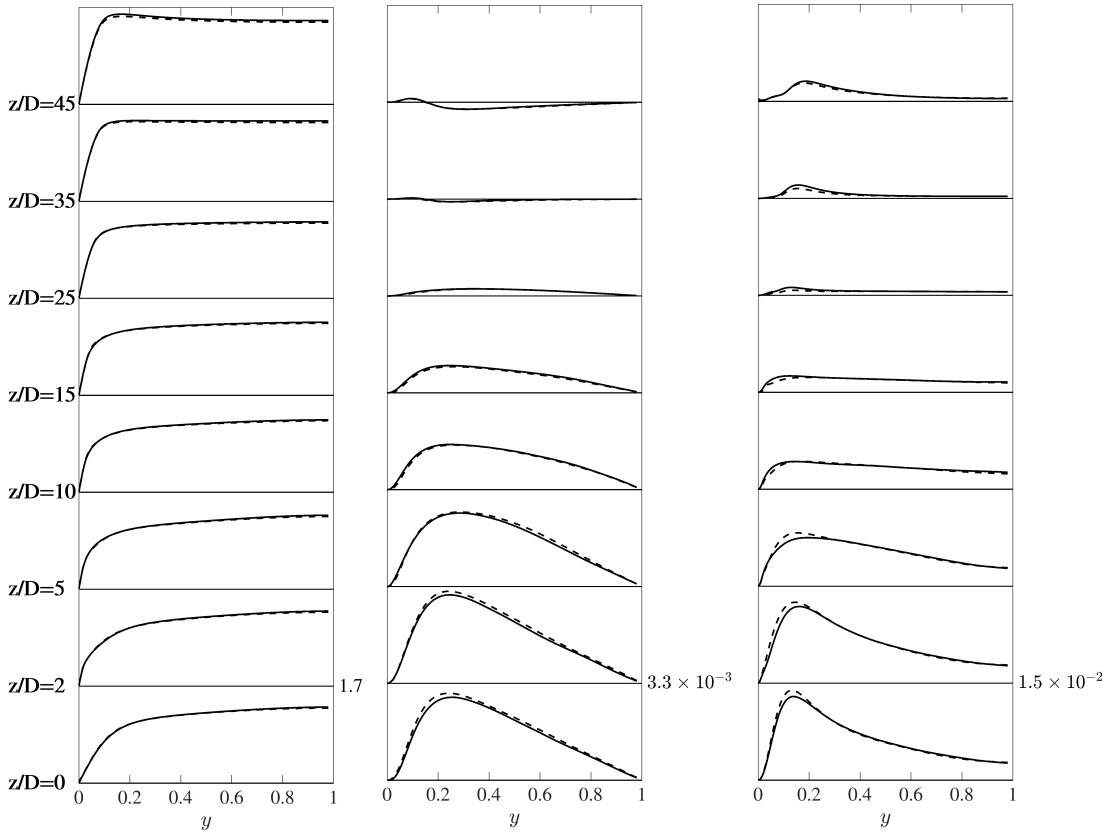

Figure 3: Radial profiles of time-averaged streamwise velocity (a), turbulent shear stress (b) and turbulent kinetic energy (c) at several chosen locations in cases NoCHT and CHT. Profiles of case NoCHT are denoted by a solid line '-' and those of case CHT are denoted by a dash line '- -'.

ρ'_{rms} profiles at $y = 0$ to 0.2 are shown. Both cases form a thermal boundary layer from about $z/D = 0$ to 5. At $z/D = 0$, case CHT has a higher enthalpy close to the wall as the fluid there is in contact with the hot solid, while for NoCHT, fluid is gradually heated by a uniform wall heat flux at the wall. Case CHT has a higher ρ'_{rms} initially as it has a much higher wall heat flux there, but at all locations except the inlet, case NoCHT has a higher ρ'_{rms}. The differences in ρ'_{rms} between the two cases are larger before $z/D = 15$ but they both reach the peak at similar radial locations. The differences between turbulent heat flux increase before z/D=5 and reduce after and case NoCHT always has a higher peak. It suggests the heat transfer between the two cases are different at early stages (about $z/D < 10$ or 15), but similar at later stages.

To identify the differences in heat transfer characteristics between the two cases, the Nusselt numbers between the two cases are compared in Figure 5a. The values both reduce significantly but differences are observed for $z/D < 10$ where the main differences of $-\overline{\rho u_r'' h''}$ are located. Here the FIK decomposition of Nu [10] is used to identify the contributing factors. The Nusselt number is decomposed into the contribution from laminar (Nu_l), turbulence (Nu_t) and flow development (Nu_{ih}). To validate the formulation of FIK decomposition, $Nu_{FIK} = Nu_l + Nu_t + Nu_{ih}$ is plotted against the the Nusselt number $Nu(z) = HTC(z)\ D^*/\lambda_b^*$ for cases NoCHT and CHT in Figure 5b & 5c, both in a good agreement. As shown in Figure 5d to 5f, before $z/D = 10$, case CHT has a stronger laminar contribution because it

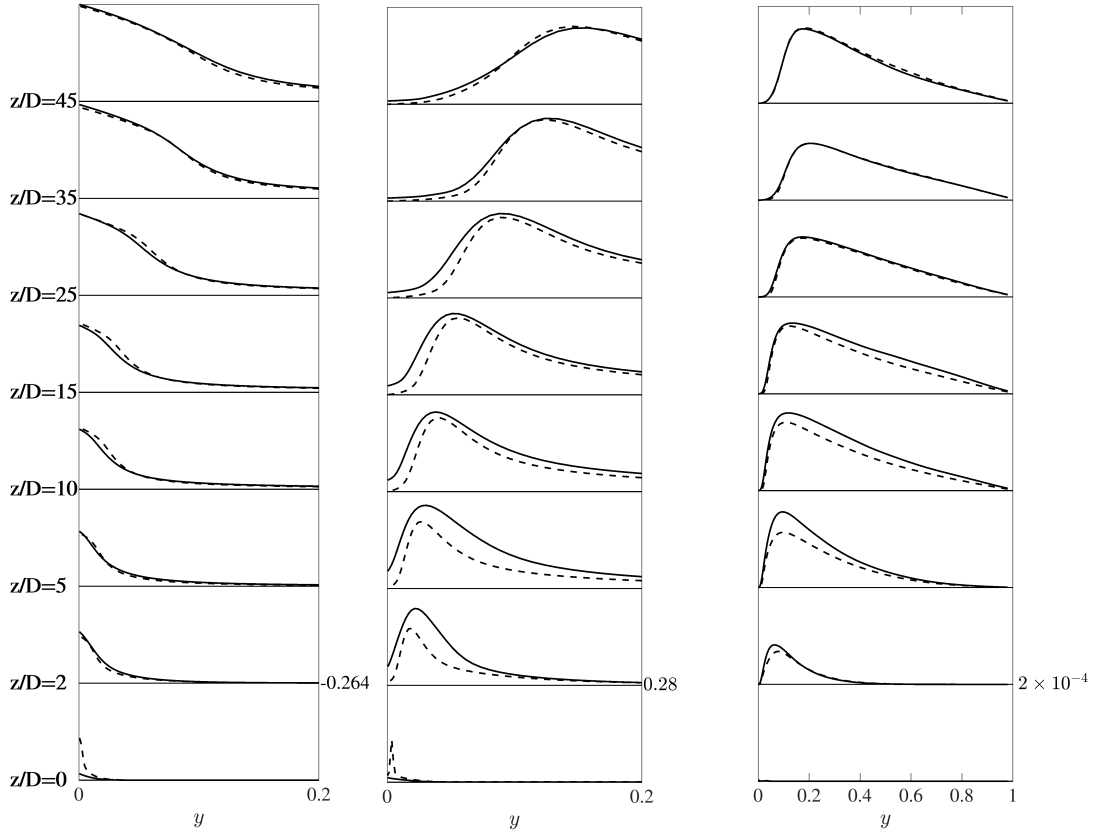

Figure 4: Radial profiles of time-averaged enthalpy (a), root-mean-square of density fluctuations (b) and radial turbulent heat flux (c) at several chosen locations in cases NoCHT and CHT. Profiles of case NoCHT are denoted by a solid line '-' and those of case CHT are denoted by a dash line '- -'.

forms a thermal boundary layer earlier. But between about $z/D = 10$ and 20, case NoCHT has a stronger turbulent contribution with a stronger turbulent heat flux. The differences in Nu_{ih} between the two is relatively small.

4 CONCLUSIONS

An investigation has been carried out to study conjugate heat transfer by comparing two upward heated pipe flows of supercritical CO_2 at $Re_0 = 3600$, with and without a solid wall. The heat transfer coefficients of the two cases agree well with experiment data after $z/D = 20$, and the wall temperatures in case CHT has the best agreement with those of the experiment. The effects of including solid wall conduction on flow development and turbulence are minor, but effect on heat transfer has been observed at early locations ($z/D < 10$). By introducing the solid wall, the laminar contribution to Nu is stronger due to a more rapid formation of the thermal boundary layer, but the turbulent contribution is weaker as the enthalpy fluctuation is dampened close to the wall. As a result, the main differences in Nu occur at $z/D < 10$ and diminish at later locations indicating a minor effect of conjugate heat transfer.

ACKNOWLEDGEMENTS

The first author gratefully acknowledges the Ph.D. studentship provided by EDF Energy. This work used the ARCHER, provided via the UKTC (EP/R029326/1). New development on CHAPSim have

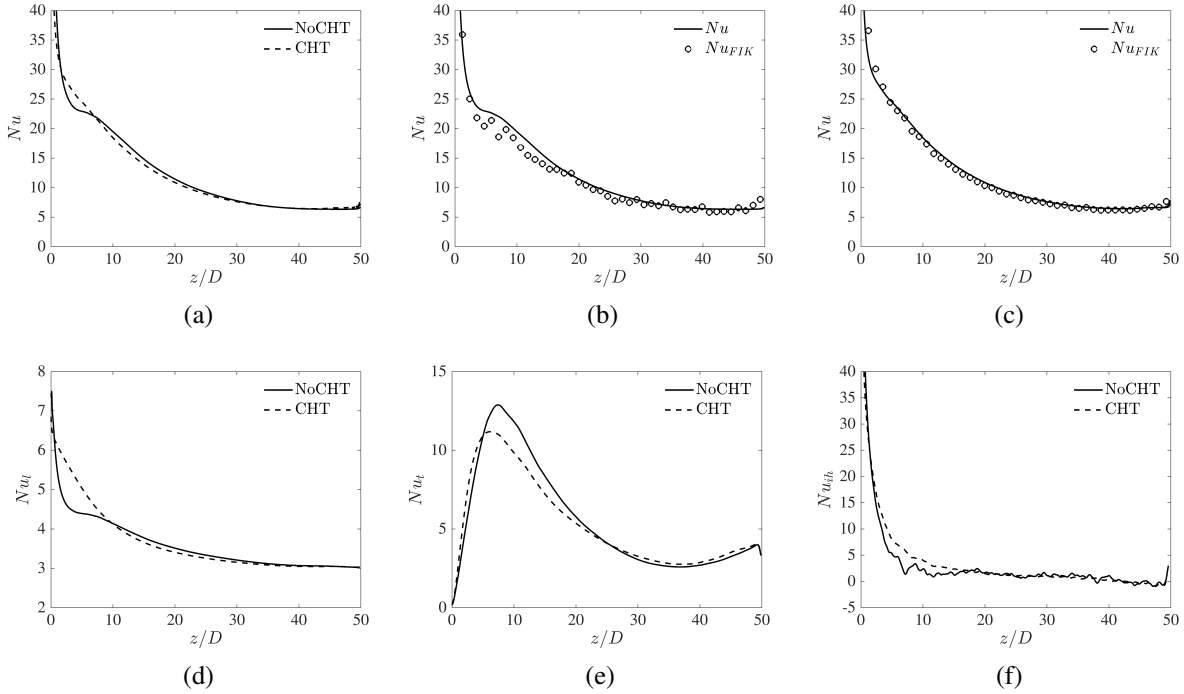

Figure 5: Nusselt number and FIK identifications of the Nusselt number in cases NoCHT and CHT: (a) Nusselt numbers; (b) Nu and Nu_{FIK} in case NoCHT; (c) Nu and Nu_{FIK} in case CHT; (d) Comparison of Nu_l; (e) Comparison of Nu_t; (f) Comparison of Nu_{ih}.

been carried out under CCP NTH (EP/T026685/1).

REFERENCES

[1] L. Feng. *Studies on flow and heat transfer involved in enhanced geothermal system and carbon dioxide utilization*. Ph.D. thesis, Tsinghua University (2014).

[2] B. Shiralkar & P. Griffith. The Effect if Swirl, Inlet Conditions, Flow Direction, and Tube Diameter on the heat Transfer to Fluids at Supercritical Pressure. *Journal of Heat Transfer*, **92** (1970) 490–497.

[3] J. Jackson. Fluid flow and convective heat transfer to fluids at supercritical pressure. *Nuclear Engineering and Design*, **264** (2013) 24–40.

[4] J. H. Bae, J. Y. Yoo, & H. Choi. Direct numerical simulation of turbulent supercritical flows with heat transfer. *Physics of fluids*, **17** (2005) 105104.

[5] J. W. Peeters, R. Pecnik, M. Rohde, T. Van Der Hagen, & B. J. Boersma. Turbulence attenuation in simultaneously heated and cooled annular flows at supercritical pressure. *Journal of Fluid Mechanics*, **799** (2016) 505–540.

[6] H. Nemati, A. Patel, B. J. Boersma, & R. Pecnik. The effect of thermal boundary conditions on forced convection heat transfer to fluids at supercritical pressure. *Journal of Fluid Mechanics*, **800** (2016) 531–556.

[7] A. Pucciarelli & W. Ambrosini. On the effect of conjugate heat transfer on turbulence in supercritical fluids: Results from a LES application. *Annals of Nuclear Energy*, **111** (2018) 340–346.

[8] S. He & M. Seddighi. Turbulence in transient channel flow. *Journal of Fluid Mechanics*, **715** (2013) 60–102.

[9] W. Wang & S. He. Mechanisms of buoyancy effect on heat transfer in horizontal channel flow. In *The 7th International Symposium on Supercritical Water-Cooled Reactors (ISSCWR-7)*, March, pp. 15–18 (2015).

[10] T. Gomez, V. Flutet, & P. Sagaut. Contribution of Reynolds stress distribution to the skin friction in compressible turbulent channel flows. *Physical Review E*, **79** (2009) 035301.